J Physiol 594.18 (2016) pp 5237–5254

The Journal of Physiology

Revisiting Frank–Starling: regulatory light chain phosphorylation alters the rate of force redevelopment (k_{tr}) in a length-dependent fashion

Christopher N. Toepfer[1,2], Timothy G. West[3] and Michael A. Ferenczi[1,4]

[1] *Molecular Medicine Section, National Heart and Lung Institute, Imperial College London, London, UK*
[2] *Laboratory of Molecular Physiology, NHLBI, National Institutes of Health, Bethesda, MD, USA*
[3] *Structure & Motion Laboratory, Royal Veterinary College London, North Mymms, UK*
[4] *Lee Kong Chian School of Medicine, Nanyang Technological University, Singapore, Singapore*

Key points

- Regulatory light chain (RLC) phosphorylation has been shown to alter the ability of muscle to produce force and power during shortening and to alter the rate of force redevelopment (k_{tr}) at submaximal [Ca^{2+}].
- Increasing RLC phosphorylation ~50% from the *in vivo* level in maximally [Ca^{2+}]-activated cardiac trabecula accelerates k_{tr}.
- Decreasing RLC phosphorylation to ~70% of the *in vivo* control level slows k_{tr} and reduces force generation.
- k_{tr} is dependent on sarcomere length in the physiological range 1.85–1.94 μm and RLC phosphorylation modulates this response.
- We demonstrate that Frank–Starling is evident at maximal [Ca^{2+}] activation and therefore does not necessarily require length-dependent change in [Ca^{2+}]-sensitivity of thin filament activation.
- The stretch response is modulated by changes in RLC phosphorylation, pinpointing RLC phosphorylation as a modulator of the Frank–Starling law in the heart.
- These data provide an explanation for slowed systolic function in the intact heart in response to RLC phosphorylation reduction.

Abstract Force and power in cardiac muscle have a known dependence on phosphorylation of the myosin-associated regulatory light chain (RLC). We explore the effect of RLC phosphorylation on the ability of cardiac preparations to redevelop force (k_{tr}) in maximally activating [Ca^{2+}]. Activation was achieved by rapidly increasing the temperature (temperature-jump of 0.5–20ºC) of permeabilized trabeculae over a physiological range of sarcomere lengths (1.85–1.94 μm). The trabeculae were subjected to shortening ramps over a range of velocities and the extent of RLC phosphorylation was varied. The latter was achieved using an RLC-exchange technique, which avoids changes in the phosphorylation level of other proteins. The results show that increasing RLC phosphorylation by 50% accelerates k_{tr} by ~50%, irrespective of the sarcomere length, whereas decreasing phosphorylation by 30% slows k_{tr} by ~50%, relative to the k_{tr} obtained for *in vivo* phosphorylation. Clearly, phosphorylation affects the magnitude of k_{tr} following step shortening or ramp shortening. Using a two-state model, we explore the effect of RLC phosphorylation on the kinetics of force development, which proposes that phosphorylation affects the kinetics of both attachment and detachment of cross-bridges. In summary, RLC phosphorylation affects the rate and extent of force redevelopment. These findings were obtained in maximally activated muscle at saturating [Ca^{2+}] and are not explained by changes in the Ca^{2+}-sensitivity of acto-myosin

DOI: 10.1113/JP272441

interactions. The length-dependence of the rate of force redevelopment, together with the modulation by the state of RLC phosphorylation, suggests that these effects play a role in the Frank–Starling law of the heart.

(Received 16 March 2016; accepted after revision 1 June 2016; first published online 13 June 2016)
Corresponding author C. N. Toepfer: Harvard Medical School, Department of Genetics, NRB-room 256, 77 Avenue Louis Pasteur, Boston, MA 02115, USA. Email: christopher_toepfer@HMS.harvard.edu

Abbreviations CF, conversion factor; DR, duty ratio; f, rate constant of cross-bridge attachment (s^{-1}); F, force produce by an individual cross-bridge (pN); $F_{1.85}$, force of a maximally activated trabecula at a sarcomere length of 1.85 μm (kN m^{-2}); $F_{1.90}$, force of a maximally activated trabecula at a sarcomere length of 1.90 μm (kN m^{-2}); $F_{1.94}$, force of a maximally activated trabecula at a sarcomere length of 1.94 μm (kN m^{-2}); F_{iso}, isometric force (kN m^{-2}); FL s^{-1}, trabecula shortening velocity (trabecula lengths s^{-1}); F_{ramp}, force sustained during a shortening ramp at a steady velocity (kN m^{-2}); F_{rec}, force recovered in isometric conditions after the end of protocol (kN m^{-2}); g, rate constant of cross-bridge detachment (s^{-1}); $k_{1.85}$, rate of force redevelopment (k_{tr}), at a sarcomere length of 1.85 μm (s^{-1}); $k_{1.90}$, rate of force redevelopment (k_{tr}), at a sarcomere length of 1.90 μm (s^{-1}); $k_{1.94}$, rate of force redevelopment (k_{tr}), at a sarcomere length of 1.94 μm (s^{-1}); k_{tr}, rate of force redevelopment (s^{-1}); N, number available cross-bridges for active cycling; RLC, regulatory light chain; SL, sarcomere length (μm).

Introduction

Contraction in striated muscle is driven by interactions between actin and myosin, and is controlled by the availability of free Ca^{2+} to bind the thin filament regulatory complex (troponin complex). This 'on/off' mechanism in striated muscle determines the availability of myosin binding sites on actin (thin filament activation) (Moss *et al.* 2004). In the presence of calcium, these sites are available and cyclical interactions between actin and myosin occur, producing force and shortening. In addition, RLC phosphorylation level plays a role in modulating the ability of cross-bridges to produce force, especially under load (Toepfer *et al.* 2013). What has not yet been well established is the ability of RLC phosphorylation to alter the kinetics of force redevelopment (k_{tr}) (not created by stretch activation) (Stelzer *et al.* 2006*a*; Stelzer *et al.* 2006*b*) in cardiac tissue. Force redevelopment was described in 1957 by Huxley using a simple two-state model, which described k_{tr} as the sum of the forward (f), and backward (g) rate constants for the transition into (and out of) the load bearing acto-myosin states, respectively (Huxley, 1957). Thus, processes that affect f or g modify the amplitude of force and the rate of force redevelopment. The amount of isometric force produced (F_{iso}) is given by:

$$F_{iso} = F \cdot N \cdot f/(f + g)$$

where F is the force per cross-bridge, N is the total number of cross-bridges in the filament overlap region and $f/(f+g)$ is the proportion of cross-bridges in force generating states.

Subsequent studies have shown that the rate constants f and g are complex terms, dependent on transitions between multiple biochemical intermediates (Pate & Cooke, 1986; Regnier *et al.* 1998). Although the two-state model does not describe the transient force response following step changes in length, it is a useful tool for making comparisons between treatment groups (Huxley & Simmons, 1971; Podolsky *et al.* 1976); for example, the rate of ADP release from the myosin active site was identified as both strain sensitive and a major determinant of g in striated muscle (Nyitrai & Geeves, 2004; Greenberg *et al.* 2014). The rate of f is dependent on thin filament activation (co-operative activation) (Bremel & Weber, 1972; Brenner, 1988; Araujo & Walker, 1994; Wolff *et al.* 1995), which in effect alters the availability of actin binding sites to which myosin heads may bind, a factor also considered to be influenced by lattice expansion or shrinkage and by regulatory light chain (RLC) phosphorylation, shifting the myosin heads closer to the thin filament by addition of a negative charge to the neck region (Barany *et al.* 1980; Ueno & Harrington, 1981; Levine *et al.* 1996; Colson *et al.* 2010). Previous studies investigating the effect of RLC phosphorylation on k_{tr} and on the stretch activation response in rat cardiac trabeculae were performed using relatively long sarcomere lengths (SL) (2.2–2.3 μm), in the presence of either limiting or maximal [Ca^{2+}], with conflicting results (Morano *et al.* 1995; Olsson *et al.* 2004; Stelzer *et al.* 2006*b*; Colson *et al.* 2010). Work on skeletal muscle in submaximal [Ca^{2+}] clearly identified RLC phosphorylation as a determinant of k_{tr} (Metzger *et al.* 1989; Sweeney & Stull, 1990). However, the role that RLC phosphorylation plays in regulating k_{tr} in cardiac muscle after shortening and at physiological sarcomere lengths observed during systole (1.91–1.68 μm) (Sonnenblick *et al.* 1967) is unknown.

By carrying out experiments in the presence of saturating [Ca^{2+}], the effect of calcium-dependent activation is eliminated such that any changes in k_{tr} depend on the RLC phosphorylation levels and not on the calcium regulatory complex (de Tombe & Stienen, 2007). The role

of RLC phosphorylation warrants investigation because the observed changes in RLC phosphorylation levels in myocardium, above or below basal levels, change both power output and force production of the tissue (Toepfer *et al.* 2013) Additionally, there is a close association between RLC phosphorylation and myocardial function, such as in disease models, both acquired and inherited (Sheikh *et al.* 2014).

In the present study, we use an *in vitro* RLC exchange protocol to alter RLC phosphorylation level in rat cardiac ventricular trabeculae, without affecting phosphorylation of other sarcomeric constituents (Toepfer *et al.* 2013). Activation of the permeabilized trabeculae is achieved by temperature-jump to ensure rapid and homogeneous activation and thereby avoiding the confounding effects of Ca-diffusion into the core of the trabeculae. We measure k_{tr} using a step release protocol at three physiological RLC phosphorylation levels that are observed in health and disease (Sheikh *et al.* 2014). This provides a measurement of absolute force redevelopment when all cross-bridges are primed to begin actively cycling after being forcibly detached by a rapid release. Measurements are carried out at three sarcomere lengths (SL, 1.94, 1.90 and1.85 μm), with the shortest being that encountered during late systole *in vivo* (Guccione *et al.* 1997; Hanft *et al.* 2008). We use release-ramp protocols to elicit force redevelopment to measure k_{tr} over a range of physiological shortening velocities that the intact myocardium would encounter during systole. This technique allows us to assess k_{tr} with unsynchronized cross-bridges populating a variety of cross-bridge states, similar to that occurring in the shortening myocardium during systole. Hence, we aim to advance our mechanistic understanding of how RLC phosphorylation alters k_{tr}, independently of calcium-dependent co-operative activation in cardiac muscle.

Methods

Ethical approval

All animal procedures were carried out in accordance with the Guide for the Care and Use of Laboratory Animals, published by the United States National Institutes of Health, under assurance number A5634-01. Cervical dislocation was performed in accordance with Schedule 1 of the UK Home Office Animals (Scientific Procedures) Act 1986.

Trabeculae preparation

Female Sprague–Dawley rats (fed *ad libitum*) weighing 250–350 g were anaesthetized using isofluorane inhalation, until unconscious. Rapid cervical dislocation was followed by removal of the heart by abdominal and subsequent thoracic resection. Hearts were excised with intact aortic arches for cannulation and retrograde perfusion with oxygenated ice-cold Krebs–Henseleit solution (composition in mM: 119 NaCl, 4.7 KCl, 0.94 $MgSO_4$, 1 $CaCl_2$, 1.2 KH_2PO_4, 25 NaHCO, 11.5 glucose and 30 2,3-butanedione monoxime, in addition to 12 units ml^{-1} of heparin). Left ventricular trabeculae (1–2 mm in length and 100–300 μm in width) were excised from the resected left ventricle. Trabeculae ends were then crimped in T-clips and pinned at resting length on Sylgard for chemical permeabilization using relaxing solution (composition in mM: 60 TES, 8.66 $MgCl_2$, 20 EGTA, 5.43 Na_2ATP, 10 glutathione and 33.71 potassium propionate at pH 7.4) for 30 min at 5°C, incorporating 2% Triton X-100. Trabeculae were stored post-permeabilization at –20°C in 50% relaxing solution with 50% glycerol and protease inhibitors (4 mg l^{-1} leupeptin, 10 mM phenylmethanesulphonyl fluoride and 50 mg l^{-1} trypsin inhibitor). Trabeculae were stored for no longer that 3 days prior to experimentation.

RLC exchange

The methods for exchange and for measuring the extent of exchange have been described previously (Toepfer *et al.* 2013). Briefly, recombinant cardiac RLC from *Rattus norvegicus* was expressed, purified and dephosphorylated or phosphorylated *in vitro* using shrimp alkaline phosphatase or smooth muscle myosin light chain kinase, respectively (Toepfer *et al.* 2013). RLCs with known phosphorylation levels (0.1 mol Pi mol^{-1} RLC, 0.5 mol Pi mol^{-1} RLC and 1.1 mol Pi mol^{-1} RLC) were exchanged for native RLC in permeabilized trabeculae using an exchange buffer (composition in mM: 5 ATP, 5 EGTA, 5 EDTA, 10 imidazole, 150 potassium propionate, 10 KH_2PO_4, 5 DTT and 0.5 trifluoperazine at pH 6.5). Exchange was performed with 0.6 mg ml^{-1} RLC on the experimental set-up at a sarcomere length of 2.1 μm at 0.5°C for 45 min. The extent of RLC phosphorylation in the trabeculae was calculated from the measured time course of RLC exchange (Toepfer *et al.* 2013). Exchange protocols were adjusted to obtain three RLC phosphorylation levels in trabeculae. These were increased phosphorylation (phosphorylated) with a normalized RLC phosphorylation of 1.5 $\pm$ 0.1 (~0.66 mol Pi mol^{-1} RLC) compared to native where the extent of phosphorylation is 0.44 mol Pi mol^{-1} RLC, reduced phosphorylation of 0.7 $\pm$ 0.05 (~0.31 mol Pi mol^{-1} RLC) and control exchange mimicking native RLC phosphorylation levels of 1.1 $\pm$ 0.1 (Toepfer *et al.* 2013).

Trabeculae mechanics

After exchange, the ends of the trabeculae were attached to the apparatus with shellac and the sarcomere length was adjusted to 2.1 μm, using the first-order sarcomere

Table 1. Experimental solutions

	Relaxing (pH 7.1)	Pre-activating (pH 7.1)	Activating (pH 7.1)
Tes	100	100	100
$MgCl_2$	7.8	6.8	6.5
Na_2ATP	5.7	5.7	5.7
EGTA	25	0.1	0
GLH	20	20	20
HDTA	0	24.9	0
CaEGTA	0	0	25

All concentrations are in mm. pH was set for the specific temperature of the solution used. GLH, glutathione; HDTA, 1,6-diaminohexane-*N*,*N*,*N*′,*N*′-tetraacetic acid.

diffraction line visualized by illumination with a HeNe laser. Contraction was triggered by a temperature-jump method where the preparation cycles through a series of solutions at high (20°C) and low (0.5°C) temperatures to activate and relax muscle contraction, respectively (Toepfer *et al.* 2013). The protocol consists of: (1) relaxing solution at 0.5°C, where no force is seen, apart from that as a result of resting tension; (2) pre-activation solution 0.5°C; (3) activating solution 0.5°C, where, at this temperature, only a little force develops (<5% of that at 20°C); (4) activating solution 20°C (shortening protocols are applied once isometric plateau is reached); and (5) and relaxing solution 20°C, where force decreases back to zero. The preparation is then returned to relaxing solution at 0.5°C and the cycle is repeated. Solution compositions are shown in Table 1. The sarcomere length was rechecked at the end of each experiment to ensure that no slippage had occurred. Each trabecula went through up to nine activation cycles without showing significant deterioration of force. Each trabecula was tested at several shortening ramp velocities (see below).

Two mechanical perturbation protocols were used in the experiments described in the present study. The first protocol consists of a rapid (step release) reduction in trabecula length, applied during the plateau of isometric force development at 20°C, starting at a sarcomere length of 2.1 μm. The speed and amplitude of the applied release is such that the trabecula becomes momentarily slack. Following the release, force re-develops. Force re-development is characterized in terms of the amplitude of force regained and the rate constant describing the speed of force redevelopment.

The second protocol, 'release-ramp', consists of a small and fast step release, followed by a slower decrease in trabecula length at a steady shortening velocity at 20°C. The step release unloads the instantaneous elasticity of the preparations and the ramp shortening allows the trabecula to reach a steady tension, which is characteristic for the ramp velocity, thus defining the force–velocity relationship. The effects of RLC phosphorylation on the force–velocity relationship have been reported previously (Toepfer *et al.* 2013). In the present study, we use the protocol to explore the redevelopment of force following the period of steady shortening. As in the 'step release' protocol, two parameters are measured: the amount of force regained and the rate of force redevelopment. Details of the two protocols are given below.

Step release protocol

Each trabecula preparation developed peak isometric force at a sarcomere length of 2.1 μm. Rapid length changes, which were faster than the maximal shortening velocity of the unloaded preparation, were applied to the trabeculae, with shortening amplitudes of –8% (end-point sarcomere length: 1.94 μm), –10% (1.90 μm) and –12% (1.85 μm) of the initial sarcomere length (2.1 μm) during activation. Isometric force redeveloped at each nominal sarcomere length, with an amplitude denoted as $F_{1.94}$, $F_{1.90}$, and $F_{1.85}$. A representative force trace for a –8% step is shown in Fig. 1*A*. Figure 1*B* shows the length transducer signal for shortenings at each of the three amplitudes. Each force recovery time-course was fit with a two-parameter exponential:

$$F = F_{rec}(1 - e^{-k_{tr}(t)})$$

where $F_r$ec is the steady-state force recovered post protocol, F is the force at time t and k_{tr} is the rate of force redevelopment post protocol.

The exponential was applied from $t = 0$, which was the time at which force was discernibly above zero ($F = 0$). This time point was when the slack had been taken up by active shortening of the trabeculae to the new lower sarcomere length (Fig. 1*C*). Figure 1*D* shows the exponential fit to three representative traces for force re-development by the same trabecula at three sarcomere lengths. The fitted rate constants were $k_{1.94} = 10\ s^{-1}$, $k_{1.90} = 9\ s^{-1}$ and $k_{1.85} = 8\ s^{-1}$. Figure 1*E* shows the scatter of residuals for the fit to plots in Fig. 1*D*. This protocol was applied to each trabecula at each RLC phosphorylation level.

Release-ramp protocol

The release-ramp protocols were designed to determine the force-velocity relationship in trabeculae for a range of RLC phosphorylation levels. A byproduct of these protocols is the time-course of force recovery following the period of shortening, which we find to be sensitive to RLC phosphorylation levels, providing information about the kinetics of actomyosin interactions. Isometric force was allowed to develop at a sarcomere length of 2.1 μm. At the plateau of isometric force, the length transducer applied a rapid shortening to the trabecula, followed by a slower shortening (Fig. 2*A*). Depending on the ramp velocity, the

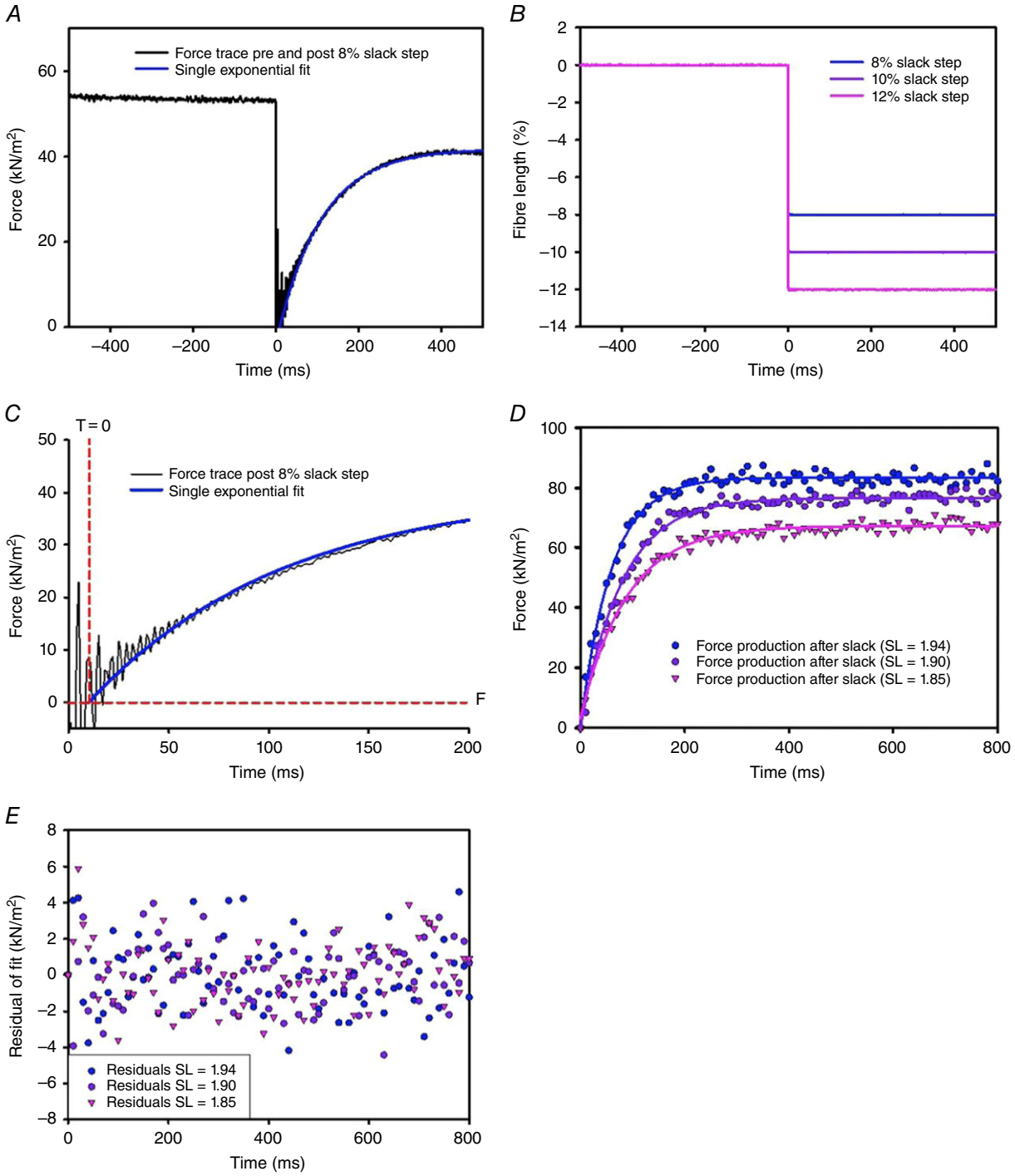

Figure 1. Step-release protocol on control trabecula
A, time course of force changes (black) of a trabecula following temperature-jump activation. Isometric force (F_{iso}) is reached before an 8% step release is applied. Force recovery after the release is fit with a single exponential (Blue & McMurray, 2005). *B*, representative motor output traces showing the step protocols for step release protocols of three different amplitudes. *C*, expanded force trace directly after step-release. Time zero is set to be the time after the end of the step release when force deviated from zero ($F = 0$). *D*, representative force recoveries observed after step releases of variable amplitude leading to different sarcomere lengths after the end of the step release. Each plot is fit with a single exponential (continuous lines). *E*, plot of residuals for each slack protocol performed in (*D*).

amplitude of the initial rapid release length was altered to minimize series elasticity during ramp, which resulted in a relatively stable force signal during ramp release (Fig. 2*D*). This protocol provides a reliable method for determining the experimental relationship between force and velocity (Curtin *et al.* 1998). Ramp velocities of 1, 0.5 and 0.3 FL s^{-1} were applied, where the velocity is expressed as fibre lengths per second (FL s^{-1}), with fibre length being the length of the trabecula between the T-clips when held at a sarcomere length of 2.1 μm. The parameters describing the length change protocols are given in Table 2.

Each protocol reduced sarcomere length by ~8% to 1.94 μm. Figure 2*B* shows representative traces of the force developing after the end of the ramp, starting at a sarcomere length of 1.94 μm. Isometric force reached after each ramp is given as F_1, $F_{0.5}$ and $F_{0.3}$, where the subscript denotes the shortening velocity during the release ramp. Figure 2*C* shows the scatter of residuals for the exponential fit to the force data in Fig. 2*B*. Figure 2*D* shows the force records during the release-ramp protocols including the subsequent force redevelopment, for trabeculae incorporating RLC at three different phosphorylation levels. The higher the phosphorylation level of the sample, the higher the force attained during initial force development at a sarcomere length of 2.1 μm (F_{iso}) and during ramp (F_{ramp}). The fit to the force recovery records after ramp shortening gave estimates for the rate constant describing the time-course of force redevelopment. The rate constants were obtained for force recovery following ramps at three different velocities (see above) and are therefore denoted k_1, $k_{0.5}$ and $k_{0.3}$ for the three ramp velocities of 1, 0.5 and 0.3 FL s^{-1}. These rate constants were calculated for each of the three phosphorylation states.

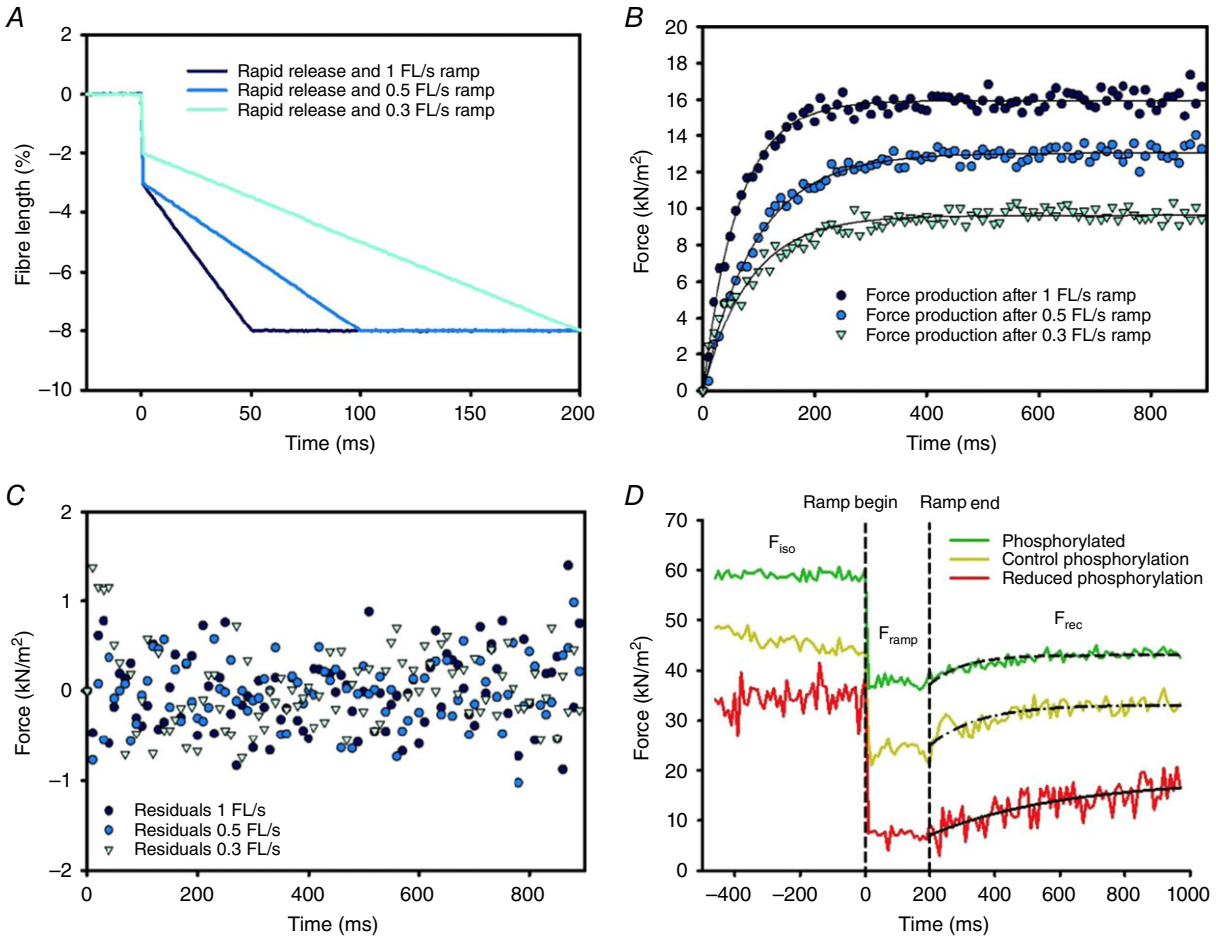

Figure 2. Release-ramp protocols
A, time course of length changes of varying speed and amplitude applied to trabeculae by the length transducer. The differences between 0.3, 0.5 and 1 FL s^{-1} release velocities are seen. *B*, time course of force recovery (F_{rec}) after release-ramp protocols of different velocities. Each force recovery is fit with a single exponential. *C*, plot of residuals for each release ramp protocol shown in (*B*). *D*, time course of force changes from three trabeculae at differing RLC phosphorylation levels, induced by the slowest ramp shown in (*A*). The force signals show that the force level during the fixed velocity ramp (F_{ramp}) depends on the RLC phosphorylation level. Phosphorylation also affects the ability of trabeculae to recover force after the end of the ramp-release (F_{rec}).

Table 2. Experimental release-ramp protocol for each ramp velocity

Ramp release (FL s^{-1})	Release amplitude (% trabecula length)	Ramp amplitude (% trabecula length)
1.0	3%	5%
0.5	3%	5%
0.3	2%	6%

All protocols released to a maximum of 8% of initial muscle length. The breakdown of the release-ramp amplitudes for each velocity protocol is shown

Modelling a two-state cross-bridge cycle

The model considers:

$$R <-> A$$

where R is the relaxed state and A is the active, force-generating state. The rate constants f and g determine transition into the force-generating state and into the relaxed state, respectively.

In such a model, the amount of force at any time (t) is given by a single exponential equation as:

$$Y = [fxN/(f + g)] \times [1 - e^{(-(f+g)\times T)}]$$

where Y is the amount of force generating cross-bridges, N is the total concentration of cross-bridges and T is time. The fraction of actin-attached cross-bridges is given by Y/N, which is also referred to as the duty ratio (DR). According to this model, the rate constant describing force generation is $(f + g)$. The rate of force development observed in the experiments described in the present study thus give estimates for $(f + g)$ under various conditions of RLC phosphorylation and sarcomere length. The observed time course of force generation is well described by a single exponential process (Fig. 1*D* and *E* and Figs 2 and 3).

For any given muscle type at full isometric activation, the DR is constant, which was approximated as 50% at control phosphorylation (He *et al.* 2000). This is 100 μm of myosin heads out of the ~200 μm available to form cross-bridges. To convert DR into a force measurement, we consider an empirical conversion factor (CF) given by:

$$\mathrm{CF} = F_{\mathrm{iso}}/\mathrm{DR}$$

The CF was assumed to be constant between RLC phosphorylation levels.

This allowed the calculation of DR for each sarcomere length and RLC phosphorylation level. Knowing k_{tr}, F_{iso} and CF allowed for the calculation of g and f as:

$$g = (\mathrm{CF} - F_{\mathrm{iso}}) \times (k_{tr}/\mathrm{CF})$$

$$f = k_{tr} - g$$

Calculating DR for each RLC phosphorylation level and SL allowed the approximation of force per cross-bridge (F_{XB}), which is given by:

$$F_{XB} = F_{\mathrm{iso}}/(\text{total heads} \times \mathrm{DR})$$

F_{XB} (in pN) and the total number of heads were derived by assuming a constant concentration of 200 μm of myosin heads (Ferenczi *et al.* 1984).

The modelling results are shown in Table 3.

Statistical analysis

We hypothesized that: (i) RLC phosphorylation and (ii) sarcomere length affected k_{tr} at maximal calcium activation. Multiple comparisons between RLC phosphorylation groups and protocols were made using two-way ANOVA to test experimental hypotheses. The hypotheses tested were (i) that SL affected k_{tr} and (ii) that RLC phosphorylation affected k_{tr}. Appropriate *post hoc* pairwise multiple comparisons were made using Bonferroni adjusted t tests, with a statistical significance cut-off of $P < 0.05$. SigmaPlot (Systat Software Inc., Chicago, IL, USA) was used to perform statistical analysis. N is the number of trabeculae sampled for each protocol. Each treatment group comprised of five cardiac preparations.

Results

The effect of RLC phosphorylation on the rate of force redevelopment and force level after step release

Measuring force redevelopment from slack allows the assessment of force production from a state where many of the cross-bridges will be synchronized in the unbound and weakly bound states (diastole). Therefore, inferences can be made about the attachment and detachment kinetics of myosin and how these parameters can be altered by SL, as well as RLC phosphorylation. Force redevelopment from slack at sarcomere lengths of 1.94 , 1.90 and 1.85 μm was measured for three different RLC phosphorylation levels (Fig. 3). These SL were used to minimize passive tension and to simulate the SL lengths that are transitioned through in late systole (Sonnenblick *et al.* 1967). For SL = 1.94 μm (Fig. 3*A*), the extent of force recovery was higher at higher levels of RLC phosphorylation, and reduced by decreasing RLC phosphorylation. Trabeculae with control levels of RLC phosphorylation produced an isometric force at a SL of 1.94 μm ($F_{1.94}$) of 63 ± 5 kN m^{-2} (Fig. 4*C*). This was not significantly different from trabeculae with increased RLC phosphorylation (78 ± 7 kN m^{-2}) but was higher than in trabeculae with reduced phosphorylation (16 ± 4 kN m^{-2}; $P < 0.05$). This was unsurprising because we have shown this phenomenon previously (Toepfer *et al.* 2013). The rate

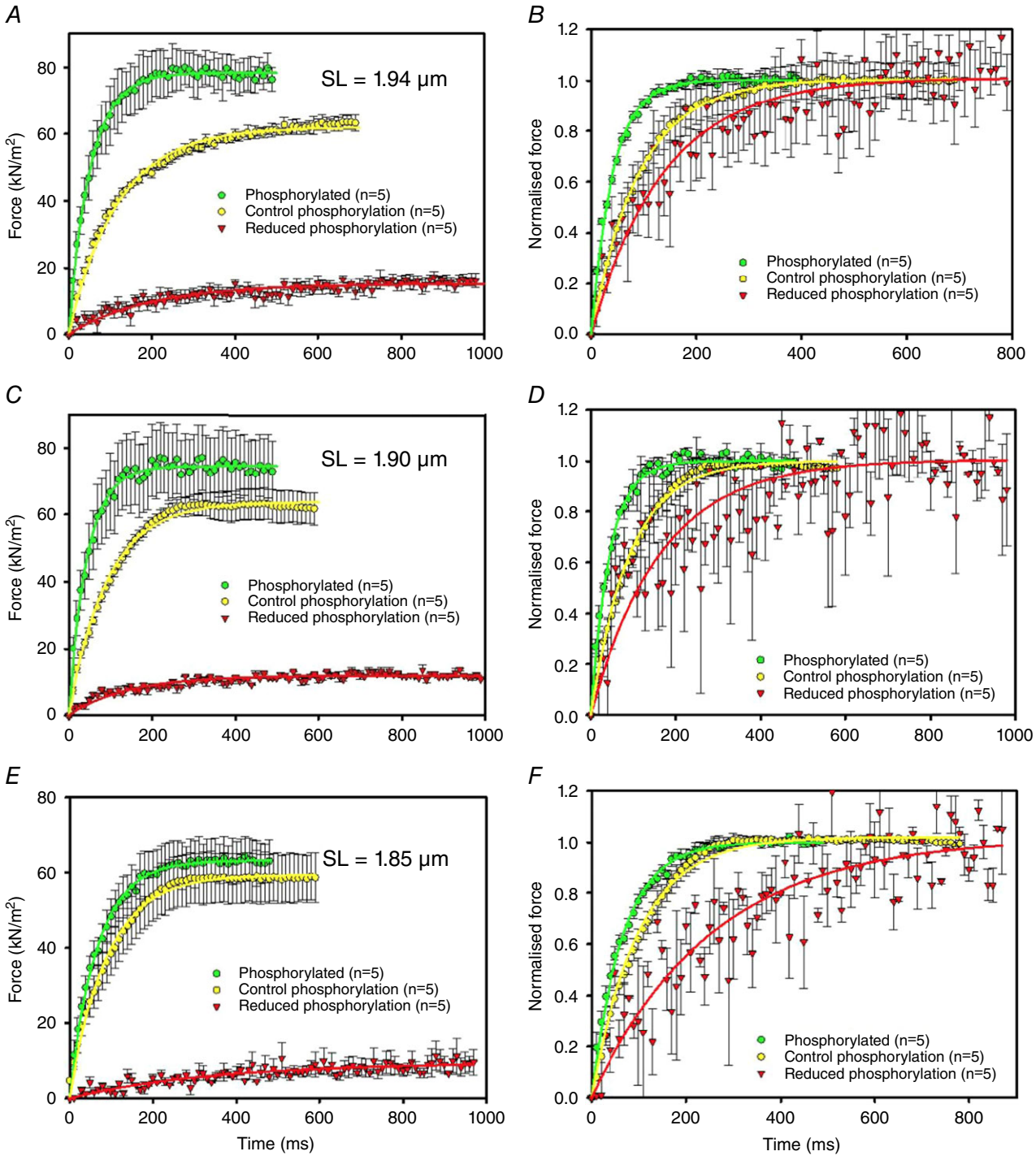

Figure 3. The effect of step release protocol on force redevelopment at three RLC phosphorylation levels

A, averaged time course of force recovery F_{rec} at SL = 1.94 μm. *B*, same records as in (*A*) after normalization for isometric force reached after force recovery. *C*, averaged time course of force recovery F_{rec} at SL = 1.90 μm. *D*, same records as in (*C*) after normalization. *E*, averaged time course of force recovery F_{rec} at SL = 1.85 μm. *F*, same records as in (*E*) after normalization. Each trace in (*B*), (*D*) and (*E*) is fitted with an exponential function to determine k_{tr}. All data points are the mean ± SEM (n = 5) and fit by a single exponential.

Table 3. Parameters from exponential fit and two state modelling of release protocol

	Phosphorylated ($n = 5$)			Control phosphorylation ($n = 5$)			Reduced phosphorylation ($n = 5$)		
Sarcomere length (μm)	1.94	1.90	1.85	1.94	1.90	1.85	1.94	1.90	1.85
F_{iso}	78 ± 7[†]	74 ± 8[†]	63 ± 6[†]	63 ± 5	60 ± 6	58 ± 7	16 ± 4	12 ± 3	8 ± 3
k_{tr} (s^{-1})	24.0 ± 1.8[*†]	22.2 ± 1.2[†]	14.9 ± 1.4[†]	11.0 ± 1.7[*]	10.7 ± 1.0	10.0 ± 0.4	7.2 ± 0.9[*]	6.1 ± 0.9	3.9 ± 1.0
Duty ratio	0.67 ± 0.05[*†]	0.59 ± 0.09[†]	0.50 ± 0.06[†]	0.50 ± 0.03[*]	0.48 ± 0.05	0.46 ± 0.07	0.13 ± 0.01[*]	0.09 ± 0.01	0.06 ± 0.02
f (s^{-1})	18.7 ± 1.4[*†]	12.9 ± 1.9[†]	7.5 ± 0.9[†]	5.5 ± 0.3	5.1 ± 0.5	4.6 ± 0.7	0.9 ± 0.1	0.6 ± 0.02	0.3 ± 0.1
g (s^{-1})	9.1 ± 0.7[*†]	9.1 ± 1.4[†]	7.5 ± 0.9[†]	5.5 ± 0.3	5.7 ± 0.5	5.4 ± 0.8	6.3 ± 0.6[*]	5.4 ± 0.2	3.7 ± 0.9
F_{XB} (pN)	3.2 ± 0.08	2.8 ± 0.16	2.8 ± 0.12	3.0 ± 0.07	3.1 ± 0.11	3.4 ± 0.19	3.1 ± 0.12	2.9 ± 0.07	3.5 ± 0.34

[*]Denotes a significant effect between SL 1.94 and 1.85 μm ($P < 0.05$).
[†]Denotesa significant effect of RLC phosphorylation within a SL length ($P < 0.05$).

constant describing force redevelopment, with a starting sarcomere length of 1.94 μm ($k_{1.94}$), was also affected by RLC phosphorylation. Unlike force, k_{tr} is affected in a dose-dependent fashion by RLC phosphorylation where control levels of RLC phosphorylation show an intermediate rate of $k_{1.94}$ 11 ± 1.7 s^{-1}, to increased and reduced phosphorylation $k_{1.94}$ 24 ± 1.8 and 7.2 ± 0.9 s^{-1} respectively, with both being significantly different from control ($P < 0.05$) (Fig. 3*B*). At the shorter sarcomere lengths of 1.90 and 1.85 μm, differences in isometric force between control trabeculae and phosphorylated trabeculae were not observed (Fig. 3*C* and *E* and Fig. 4*C*). However, in both instances, trabeculae with reduced RLC phosphorylation exhibited a significantly lower force when compared to control and phosphorylated samples at a SL of 1.94 μM ($P < 0.05$). Phosphorylation level similarly affected the rate of force redevelopment at shorter sarcomere lengths in a manner the same as that for the longer starting sarcomere length of 1.94 μm ($P < 0.05$) (Fig. 4). Therefore, the affect of RLC phosphorylation on k_{tr} is an independent modulator of k_{tr}, which is not altered by SL in this range. Strikingly, at a sarcomere length of 1.85 μm, trabeculae with reduced RLC phosphorylation (70% of control) generated only a small amount of force (10–15%) compared to the values at control and 150% phosphorylation. ($P < 0.05$). The reason for this effect is unclear. However, reducing RLC phosphorylation reduces the ability of muscle to generate force at full thin filament activation, indicating that either force per cross-bridge or cross-bridge formation is significantly hindered.

Normalizing to the isometric force at each sarcomere length highlights the effect of RLC phosphorylation on k_{tr} by allowing a direct comparison of the time-course of force redevelopment at each phosphorylation level (Fig. 3*B*, *D* and *F*). This highlights the role of RLC phosphorylation on force redevelopment at the three physiological sarcomere lengths tested (Fig. 4*A*).

Additionally, for each RLC phosphorylation level, k_{tr} is slower at shorter sarcomere lengths (Fig. 4*B*). The gradients of linear regressions applied to the data in Fig. 4*B* were 79 ± 14, 8 ± 0.2 and 26 ± 3 s^{-1} μm^{-1} for phosphorylated, control phosphorylation and reduced phosphorylation, respectively ($n = 5$). Statistical significance was observed between each slope ($P < 0.05$).

The effect of RLC phosphorylation on the rate of force production and extent of redeveloped force after release-ramp protocols

Trabeculae with one of three different RLC phosphorylation levels underwent release-ramp shortening protocols during activation at 20°C to a final sarcomere length of 1.94 μm (8% total shortening). Release-ramp shortening simulates active cross-bridge cycling at different muscle loads, which would be

encountered during systole. At the end of these manoeuvres, force redevelopment occurs in mixed populations of cross-bridge states, unlike the release protocol, which synchronizes all myosin heads into weakly (or unbound) states. This assay allows us to assess whether changes in k_{tr} can be attributed to enhanced thin filament activation by already bound cross-bridges. The shortening velocities were 1, 0.5 and 0.3 FL s^{-1} (Fig. 5*A*, *C* and *E*), where 0.3 redevelops force from the highest muscle load with the most attached cross-bridges, by proportion. For each RLC phosphorylation level, F_{iso} was constant across all ramp velocities (Fig. 6*C*). This was expected because F_{iso} was attained at a SL length of 1.94 μm after each manoeuvre velocity. Trabecular preparations with reduced RLC phosphorylation displayed a reduced F_{iso} post release (independently of release velocity) of 19 ± 2 kN m^{-2} ($P < 0.05$) versus control of 49 ± 4 kN m^{-2} and phosphorylated of 55 ± 3 kN m^{-2} (Fig. 6*C*).

Normalizing force development at each RLC phosphorylation level for each ramp velocity illustrates the effect of RLC phosphorylation on the rate of force rise (Fig. 5*B*, *D* and *F*). Trabeculae with control

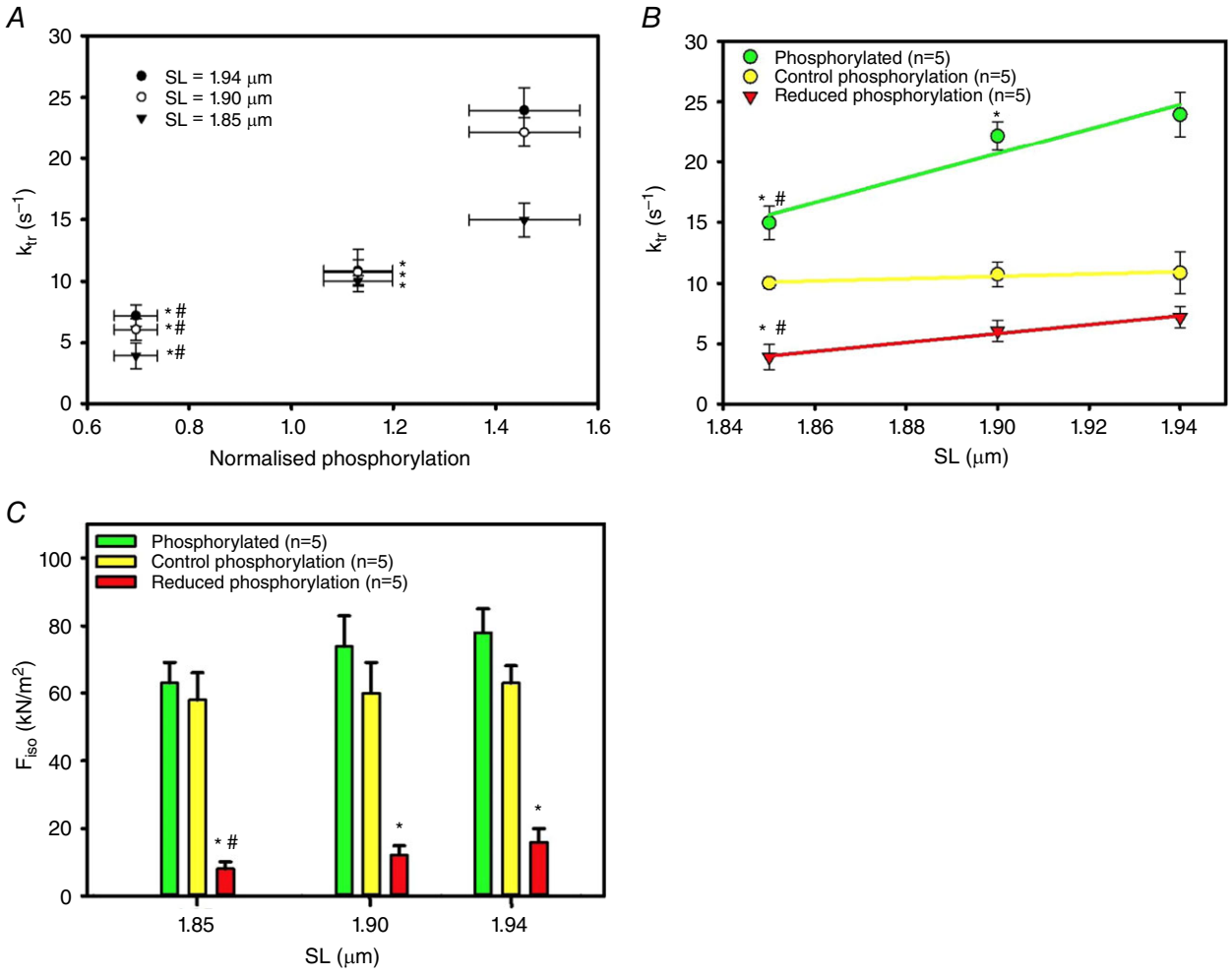

Figure 4. The effect of RLC phosphorylation on k_{tr} following the step-release protocol
A, plot of k_{tr} as a function of normalized RLC phosphorylation at three sarcomere lengths. Reduced phosphorylation is 0.69 ± 0.04, control phosphorylation is 1.13 ± 0.07 and phosphorylated is 1.45 ± 0.1. *Significant difference compared to phosphorylated, where $P < 0.05$. #Significant difference compared to control phosphorylation where $P < 0.05$. *B*, plot of k_{tr} as a function of sarcomere length (SL) for three different RLC phosphorylation levels. Data are the mean ± SEM. Linear regression is used to fit k_{tr} as a function of sarcomere length data ($n = 5$ for each point). The slopes of the regressions are 79 ± 14, 8 ± 0.2 and 26 ± 3 s^{-1} μm^{-1} for phosphorylated, control phosphorylation and reduced phosphorylation, respectively ($n = 5$). Significance was achieved between each slope, where $P < 0.05$. *Significant difference compared to 1.94 μm, where $P < 0.05$. #Significant difference compared to 1.90 μm, where $P < 0.05$. *C*, bar graph depicting F_{iso} for each RLC phosphorylation level at each sarcomere length. *Significant difference compared to control phosphorylation (and phosphorylated) within SLs, where $P < 0.05$. #Significant difference compared to corresponding phosphorylation levels at 1.94 μm, where $P \leq 0.05$.

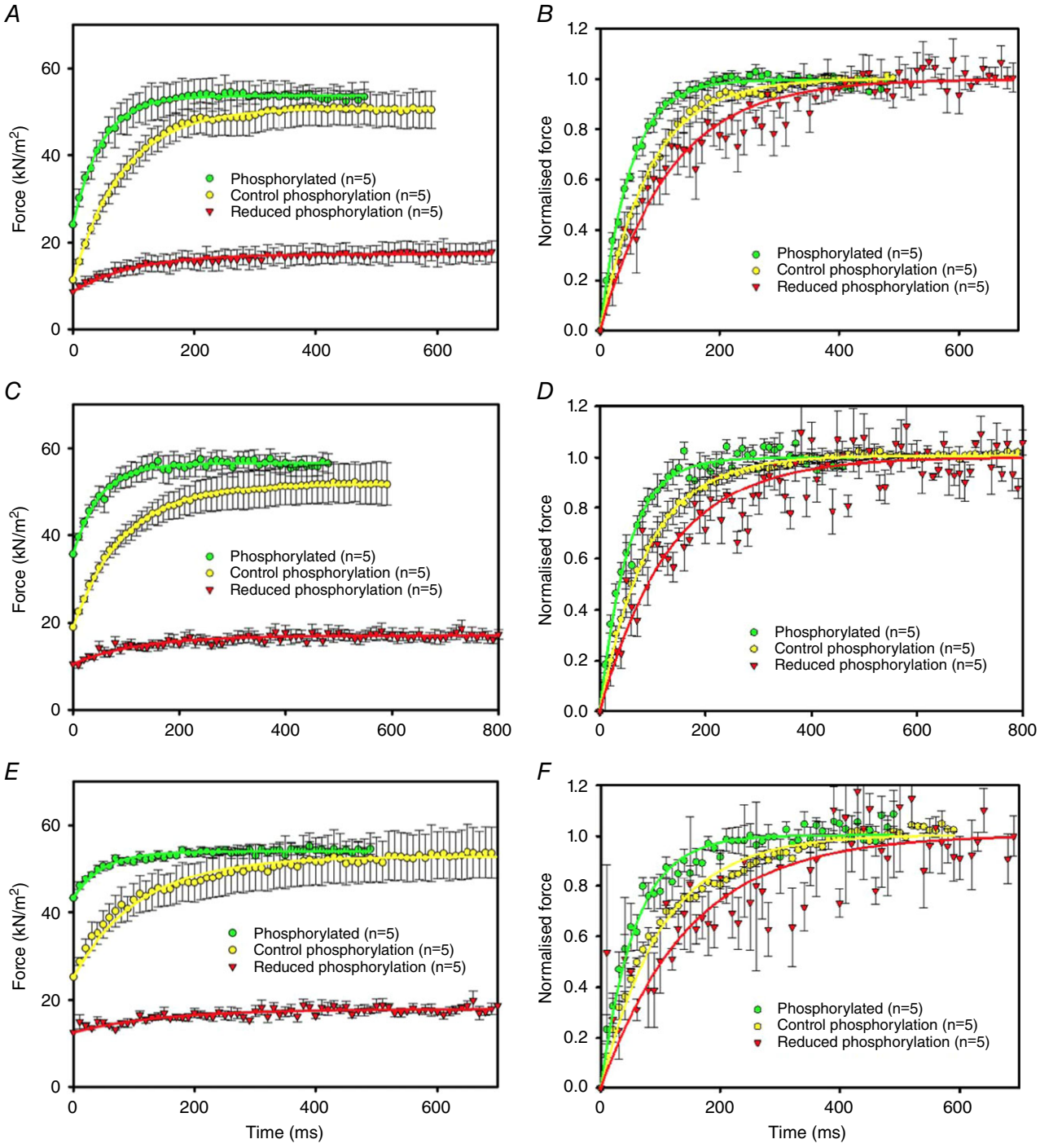

Figure 5. The effect of RLC phosphorylation levels on k_{tr} in release-ramp protocols on force redevelopment at three RLC phosphorylation levels
A, time course of force redevelopment F_{rec} after shortening at 1 FL s^{-1}. *B*, the same records as in (*A*) after normalization. *C*, time course of force redevelopment F_{rec} after shortening at 0.5 FL s^{-1}. *D*, The same records as in (*C*) after normalization. *E*, time course of force redevelopment F_{rec} after shortening at 0.3 FL s^{-1}. *F*, the same records as in (*E*) after normalization. Each trace in (*B*), (*D*) and (*E*) is fitted with an exponential function to determine k_{tr}. All data points are the mean ± SEM ($n = 5$) and fit by single exponential.

RLC phosphorylation displayed rate constants for force production of 12 ± 1.2, 11 ± 1.1 and 10 ± 0.5 s^{-1} at velocities of 1, 0.5 and 0.3 FL s^{-1} respectively (Fig. 6*B* and Table 4). Force rose more quickly for trabeculae with increased RLC phosphorylation compared to control ($P < 0.05$) at 21 ± 1.6, 19 ± 1.7 and 18 ± 1.6 s^{-1} for velocities of 1, 0.5 and 0.3 FL s^{-1}, respectively. Trabeculae with reduced RLC phosphorylation had slower rates of force production compared to control ($P < 0.05$) with rates of 10 ± 3.2, 7.6 ± 0.8 and 6.7 ± 1.1 s^{-1} at velocities of 1, 0.5 and 0.3 FL s^{-1}, respectively.

Clearly, k_{tr} is altered by RLC phosphorylation level change at saturating [Ca^{2+}] (Fig. 6*A* and Table 4). The effect is seen for force redevelopment after ramp shortening at all ramp velocities, although the effect of ramp velocity itself is small and does not reach statistical significance. This may infer that additional thin filament activation by cross-bridge binding is either a small or insignificant effector of k_{tr} in this assay, and that changes in k_{tr} are associated with mechanisms involving thick filament regulation and not thin filament regulation under these experimental conditions.

Discussion

RLC phosphorylation is known to be important in many elements of cardiac physiology and disease, including in cardiac developmental organization (Nishio *et al.* 1997;

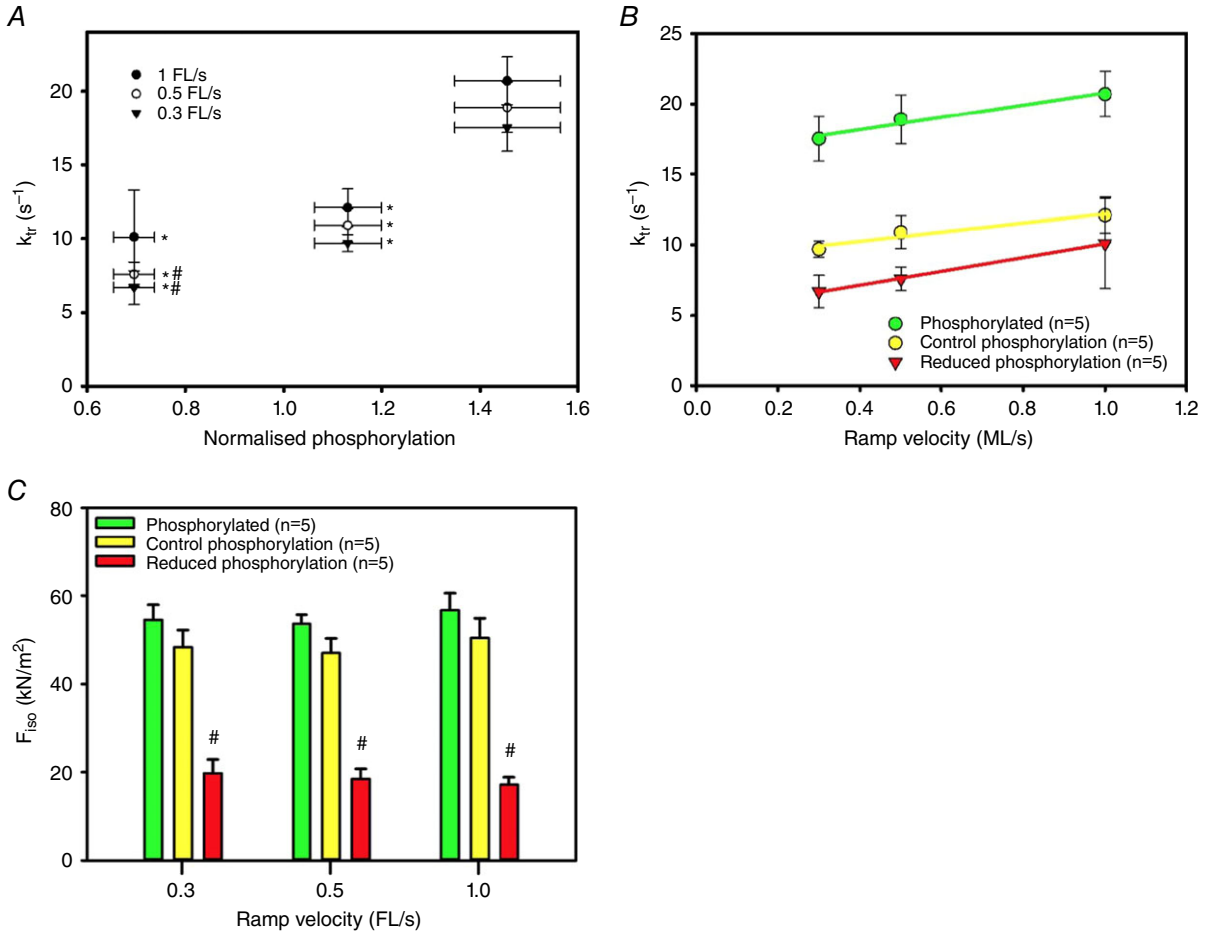

Figure 6. The effect of RLC phosphorylation on k_{tr} following the release-ramp protocol
A, the rate of force redevelopment k_{tr} as a function of normalized RLC phosphorylation at SL = 1.94 μm following ramp shortening at three velocities. Reduced phosphorylation is 0.69 ± 0.04, control phosphorylation is 1.13 ± 0.07 and phosphorylated is 1.45 ± 0.1. *Significant difference compared to phosphorylated, where $P < 0.05$. #Significant difference compared to control phosphorylation, where $P < 0.05$ *B*, the rate of force redevelopment k_{tr} as a function of shortening velocity for three different RLC phosphorylation levels. Data are shown as the mean ± SEM ($n = 5$). There are no significant differences within RLC phosphorylation levels. Linear regression is used to fit k_{tr} as a function of ramp velocity data. There are no significant differences between the slopes. *C*, bar graph depicting F_{iso} for each RLC phosphorylation level after each ramp velocity. *Significance between all RLC phosphorylation levels at a specific velocity, where $P < 0.05$. #Significant difference compared to corresponding phosphorylation levels at 1 FL s^{-1}, where $P < 0.05$.

Table 4. Parameters from exponential fit of release-ramp protocol

	Phosphorylated ($n = 5$)			Control phosphorylation ($n = 5$)			Reduced phosphorylation ($n = 5$)		
Release velocity (μm)	0.3	0.5	1	0.3	0.5	1	0.3	0.5	1
F_{iso}	55 ± 3†	54 ± 2†	57 ± 4†	49 ± 4	47 ± 3	50 ± 4	19 ± 2	18 ± 2	17 ± 2
k_{tr}	18 ± 1.6†	19 ± 1.7†	21 ± 1.6†	10 ± 0.5	11 ± 1.1	12 ± 1.2	6.7 ± 1.1	7.6 ± 0.8	10 ± 3.2

†Denotes a significant effect of RLC phosphorylation within a SL length ($P < 0.05$).

Okamoto *et al.* 2006), in regulation of ventricular torsion (Davis *et al.* 2001; Hidalgo *et al.* 2006), and in acquired (Aoki *et al.* 2000; Gu *et al.* 2010) and inherited diseases (Sanbe *et al.* 1999; Ding *et al.* 2010; Sheikh *et al.* 2012; Warren *et al.* 2012). Of note, the atria and ventricles have separate isoforms of the RLC, and different mammals have different RLC sequences with different numbers of phosphorylatable residues. Accordingly, care needs to be taken when comparing results from different species (Morano, 1992).

We have previously demonstrated the ability of RLC phosphorylation to influence myocardial force production, power and shortening under-load (Toepfer *et al.* 2013). Previous studies have probed the effect of RLC phosphorylation on k_{tr}, but have not assessed physiological sarcomere lengths, and have shown conflicting results (Olsson *et al.* 2004; Colson *et al.* 2010). In the present study, we add clarity by showing that, at maximal activation, RLC phosphorylation and, to a lesser extent, sarcomere length alter k_{tr}. The observed changes are consistent with the Frank–Starling law of the heart and may indicate a new mechanism that contributes to this phenomenon (discussed below). Importantly, our measurements at saturating calcium allow us to consider processes that are independent of the Ca^{2+}-dependent contributions to the Frank–Starling law, and also show that RLC phosphorylation and the thick filament contribution both play a role in the Frank–Starling law.

The effect of sarcomere length on the rate of force production

Our measurements of k_{tr} in control phosphorylation are in the range observed in previous studies at maximal activation between ∼4.5 and 14 s^{-1} with variance as a result of changes in temperature and muscle type (Wolff *et al.* 1995; Fitzsimons *et al.* 2001; Regnier *et al.* 2004). Additionally, k_{tr} at control phosphorylation levels (10–11 s^{-1}) is close to the ATPase rate in trabeculae from rats under identical experimental conditions (∼8 s^{-1}) (Mansfield *et al.* 2012).

Increasing sarcomere length from ∼1.85 to 1.94 μm accelerated k_{tr} at each RLC phosphorylation level. The acceleration of k_{tr} with stretch, independently of $[Ca^{2+}]$, is observed in intact myocardium (Rhodes *et al.* 2015) and is a calcium independent manifestation of length-dependent activation (de Tombe *et al.* 2010). This is in agreement with the length–tension relationship of trabeculae from rat because the sarcomere lengths used in the present study are in the ascending limb of the length–tension curve (Kentish *et al.* 1986). Some previous studies have shown that k_{tr} decreased between SLs of 2.0 and 2.35 μm (Korte & McDonald, 2007; Patel *et al.* 2012) or had no statistical effect (Adhikari *et al.* 2004; Hanft & McDonald, 2010), as well as between 2.0 and 2.2 μm (Milani-Nejad *et al.* 2013). The differences between these findings and those reported in the present study could conceivably be a result of the SLs assessed or the technique used to assess k_{tr} because the aforementioned studies used restretch protocols. The common interpretation of the Frank–Starling law is that, with higher pre-loads, the myocardium develops a greater systolic force as a result of calcium-sensitive length-dependent activation, as well as changes in myofilament overlap (Katz, 2002; de Tombe *et al.* 2010). In accordance with Frank–Starling, our data suggest that the force of contraction increases with pre-load (an increased stretch of myocardium as a result of increased chamber volume is accompanied by increases in SL). Additionally, our data show that the rate at which force is produced is also affected, although this phenomenon only appears to be evident in situations where RLC phosphorylation is raised or lowered from control levels (Table 3). This phenomenon is beneficial to the ejection fraction because the systolic duration would not need to be prolonged to fully accommodate extra expulsion: k_{tr} accelerates to compensate for increased ejection volume. Because this effect is observed at saturating $[Ca^{2+}]$, it is independent of calcium-sensitive activation and the thin filament regulatory complex. Thus, the measured changes in k_{tr} are explained by direct interactions between myosin and actin that are independent of thin filament activation and may be a consequence of the increase in f, which will alter the distribution of actomyosin states towards strongly-bound, force-generating states.

The effect of RLC phosphorylation on the rate of force production

Our results show that RLC phosphorylation level alters k_{tr} over a range of SLs (1.85–1.94 μm) during maximal calcium activation, in contrast to the findings of another study at a higher SL (∼2.3 μm), which observed no

change to k_{tr} at this higher SL (Olsson *et al.* 2004). The difference in experimental result is probably a result of the aforementioned differences in SL, possibly because k_{tr} is influenced by inter filament spacing, which is altered by the length of the muscle (Wang & Fuchs, 1995). Our measurements at the shorter, physiological sarcomere lengths are probably more meaningful during systole (Sonnenblick *et al.* 1967), although saturating $[Ca^{2+}]$ and the less than physiological temperature may also influence the ability to extrapolate our findings to the situation in the living animal.

Our measurements are made in saturating $[Ca^{2+}]$; therefore, RLC phosphorylation must be altering cross-bridge behaviour independently of the thin filament regulatory complex. Consequently, RLC phosphorylation modulates the Frank–Starling law of the heart (although not on a beat to beat basis) (Stracher, 1969). We propose that RLC phosphorylation level is another mechanism by which the myocardium modulates its ability to redevelop force in response to increased ventricular pre-load.

Interestingly, under chronic raised pre-load, RLC phosphorylation is raised as a compensatory mechanism to greater ventricular volume (Hidalgo *et al.* 2006), providing further evidence that RLC phosphorylation is an important modulator of systolic ejection in the intact organ. Additionally, experimental models with reduced RLC phosphorylation display increased systolic duration and slowed cross-bridge kinetics, in accordance with our findings (Abraham *et al.* 2009; Scruggs *et al.* 2009). The use of constitutive RLC pseudophosphorylation to correct RLC phosphorylation reduction has been shown to alleviate this phenomenon (Yuan *et al.* 2015). By contrast, hyperphosphorylation of RLC increases contractility and contractile efficiency independently of any disease phenotype (Huang *et al.* 2008). Together, these findings are complementary to our own. Dephosphorylation of RLC slows $k_{tr,}$ which prolongs systole: pre-load ejection takes longer because systolic contractile kinetics are slowed. Similarly a raised k_{tr} as a result of RLC phosphorylation explains increased ejection characteristics as cross-bridge recruitment is accelerated by RLC phosphorylation.

Modelling of cross-bridge attachment (*f*) and detachment (g)

We note that the rate of force redevelopment, k_{tr}, was well described by fitting a single exponential to the force signal (Brenner, 1986; Metzger *et al.* 1989; de Tombe & Stienen, 2007). This justifies the application of a simple two-state model to delve into the attachment and detachment kinetics giving rise to the measurable k_{tr}. In the two-state model of the cross-bridge cycle, k_{tr} is represented by the sum of the two rate constants, f and g (Huxley, 1957). Although the two-state model is a simplistic approximation to cross-bridge behaviour (Huxley & Simmons, 1971; Podolsky *et al.* 1976), it is a useful tool for exploring the effect of RLC phosphorylation. Modelling of control tissue resulted in values of f and g that are comparable to previous studies reported in the literature (Brenner, 1988; Prakash *et al.* 1999; Prakash *et al.* 2000). The model provides values for f, g, DR and F_{XB}, which describe our experimental findings (Table 3).

The modelling suggests that RLC phosphorylation accelerates f, probably as result of a closer myosin head proximity to actin (Levine *et al.* 1996; Colson *et al.* 2010). The model also calculates a modest acceleration of g with increasing RLC phosphorylation. Changes to g manifest as changes in the ratio between ATPase and isometric force (Huxley, 1957). Indeed, it was shown that myosin light chain kinase treatment increased myosin ATPase and did not alter isometric force, in keeping with this modelling outcome (Muthu *et al.* 2012). At higher RLC phosphorylation, g is accelerated and the peak isometric force was stable. The modelling outcome is supported experimentally as the acceleration of f must be greater than the acceleration of g, otherwise isometric force would fall as phosphorylation increases (Regnier *et al.* 2000). When comparing trabeculae with reduced and increased phosphorylation, the rate of f is accelerated ~20 fold at each SL, whereas g is only accelerated ~1.6 fold. A recent study suggests that RLC phosphorylation slows cross-bridge detachment (g), which does not fit the modelling of our experimental data and contradicts the existing literature (Pulcastro *et al.* 2016). The discrepancy may result from the different experimental and modelling approaches for the study of cross-bridge kinetics. The lack of experimental records in this publication, as well as the apparent very low isometric force, makes it difficult to explore the source of the discrepancy. Perhaps the phosphorylation state of other sarcomeric proteins is also different from that achieved in the present study (Pulcastro *et al.* 2016).

In our experiments, reduced RLC phosphorylation levels are accompanied by reductions in F_{iso} and k_{tr}. The relative reduction of F_{iso} in the trabeculae with reduced RLC phosphorylation compared to control is greater (~75%) than the reduction in k_{tr} (~30%). This may be accounted for by a shift towards the super relaxed state of the myosin heads (Hooijman *et al.* 2011), reducing N. It is probable that either one (or both) of f and the myosin ATPase rate must be altered by reduced RLC phosphorylation to account for this reduction of force. Our modelling estimates a marked ~5-fold reduction in f in the reduced phosphorylation cohort, which, again, is probably explained by myosin proximity to actin (Colson *et al.* 2010).

Our findings cannot rule out the possibility of additional thin filament co-operativity induced by myosin binding, even in the presence of saturating calcium (Regnier *et al.* 2004). Similarly, acceleration of force

redevelopment may well be achieved by other mechanisms that affect *f*, such as the unitary force of each cross-bridge and the neck region stiffness, or indeed a change in the size of the working stroke under load, which cannot be accounted for by a two-state model (Nyitrai & Geeves, 2004; Greenberg *et al.* 2009; Karabina *et al.* 2015). Our modelling suggests that F_{XB} is not altered by RLC phosphorylation. However, this could be an unavoidable artefact of necessary assumptions in our modelling; namely, *N* remains constant at each RLC phosphorylation level, which we cannot directly address in the present study. However, in skeletal muscle, it was found that F_{XB} and *N* were not altered by phosphorylation, which may also translate to cardiac muscle (Sweeney & Stull, 1990). Our calculated value of F_{XB} is comparable to that calculated previously in other studies: 1.25–7 pN with an average of ∼3 pN between these studies, which is in good agreement with our approximation from modelling (Ishijima *et al.* 1996; Takagi *et al.* 2006) (Ishijima *et al.* 1996; Nag *et al.* 2015).

A striking finding of our modelling is that SL affected k_{tr}, *f* and *g*; additionally, stretch influenced the transition from weakly to strongly bound cross-bridges more than the transition from strongly to weakly bound. This asymmetry suggests a role for lattice spacing effects. Bringing myosin heads closer to actin accelerates *f* at the same time as having a smaller effect on *g*.

The findings of the model reported in the present study are compatible with our previous findings using force velocity and power velocity relations to assess the effect of RLC phosphorylation on cardiac contractile output (Toepfer *et al.* 2013). The finding that RLC phosphorylation accelerates the transition from weakly to strongly bound cross-bridges is compatible with the observed increase in force and power produced during shortening, as well as with the increase in maximal unloaded shortening velocity seen with enriched RLC phosphorylation (Toepfer *et al.* 2013).

In the context of twitch contractions at lower physiological calcium activations in the myocardium, an increasing RLC phosphorylation may increase the calcium sensitivity of contraction and create greater thin filament activation at lower calcium levels. This would be mediated by co-operative activation of the thin filament created by RLC phosphorylation, allowing for the faster attachment of cross-bridges. Additional studies should aim to investigate this effect in submaximal calcium concentrations with this experimental system.

Conclusions

Under conditions where myosin heads are largely synchronized (post rapid release protocol) or unsynchronized (post release ramp protocol), RLC phosphorylation alters k_{tr}. SL alters k_{tr} on a beat-to-beat basis because it is affected by ventricular pre-load causing myocardial stretching. RLC phosphorylation adds another level of regulation on k_{tr}, which is observed under chronic conditions of pre-load, which probably comprises a more long-term mechanism for fine-tuning myocardial contractility. In models of disease that are caused by reductions in RLC phosphorylation, the phenotype of ineffectual muscle contraction is brought about by reduced cross-bridge cycling rates and a reduction in actively cycling cross-bridges (*N*). Our results complement these findings, highlighting RLC phosphorylation as being a thick filament level regulator of the Frank–Starling law of the heart, which is independent of the thin filament regulatory complex. We suggest that RLC phosphorylation modulates the Frank–Starling law of the heart in both health and disease. It does so by adapting myocardial contractile kinetics, allowing for the timely systolic expulsion of ventricular pre-load.

References

Abraham TP, Jones M, Kazmierczak K, Liang HY, Pinheiro AC, Wagg CS, Lopaschuk GD & Szczesna-Cordary D (2009). Diastolic dysfunction in familial hypertrophic cardiomyopathy transgenic model mice. *Cardiovasc Res* **82**, 84–92.

Adhikari BB, Regnier M, Rivera AJ, Kreutziger KL & Martyn DA (2004). Cardiac length dependence of force and force redevelopment kinetics with altered cross-bridge cycling. *Biophys J* **87**, 1784–1794.

Aoki H, Sadoshima J & Izumo S (2000). Myosin light chain kinase mediates sarcomere organization during cardiac hypertrophy in vitro. *Nat Med* **6**, 183–188.

Araujo A & Walker JW (1994). Kinetics of tension development in skinned cardiac myocytes measured by photorelease of Ca^{2+}. *Am J Physiol Heart Circ Physiol* **267**, H1643–H1653.

Barany K, Barany M, Gillis JM & Kushmerick MJ (1980). Myosin light chain phosphorylation during the contraction cycle of frog muscle. *Fed Proc* **39**, 1547–1551.

Blue L & McMurray J (2005). How much responsibility should heart failure nurses take? *Eur J Heart Fail* **7**, 351–361.

Bremel RD & Weber A (1972). Cooperation within actin filament in vertebrate skeletal muscle. *Nat New Biol* **238**, 97–101.

Brenner B (1986). The cross-bridge cycle in muscle. Mechanical, biochemical, and structural studies on single skinned rabbit psoas fibres to characterize cross-bridge kinetics in muscle for correlation with the actomyosin-ATPase in solution. *Basic Res Cardiol* **81** (Suppl 1), 1–15.

Brenner B (1988). Effect of Ca^{2+} on cross-bridge turnover kinetics in skinned single rabbit psoas fibres: implications for regulation of muscle contraction. *Proc Natl Acad Sci USA* **85**, 3265–3269.

Colson BA, Locher MR, Bekyarova T, Patel JR, Fitzsimons DP, Irving TC & Moss RL (2010). Differential roles of regulatory light chain and myosin binding protein-C phosphorylations in the modulation of cardiac force development. *J Physiol* **588**, 981–993.

Curtin NA, Gardner-Medwin AR & Woledge RC (1998). Predictions of the time course of force and power output by dogfish white muscle fibres during brief tetani. *J Exp Biol* **201**, 103–114.

Davis JS, Hassanzadeh S, Winitsky S, Lin H, Satorius C, Vemuri R, Aletras AH, Wen H & Epstein ND (2001). The overall pattern of cardiac contraction depends on a spatial gradient of myosin regulatory light chain phosphorylation. *Cell* **107**, 631–641.

de Tombe PP, Mateja RD, Tachampa K, Ait Mou Y, Farman GP & Irving TC (2010). Myofilament length dependent activation. *J Mol Cell Cardiol* **48**, 851–858.

de Tombe PP & Stienen GJ (2007). Impact of temperature on cross-bridge cycling kinetics in rat myocardium. *J Physiol* **584**, 591–600.

Ding P, Huang J, Battiprolu PK, Hill JA, Kamm KE & Stull JT (2010). Cardiac myosin light chain kinase is necessary for myosin regulatory light chain phosphorylation and cardiac performance in vivo. *J Biol Chem* **285**, 40819–40829.

Ferenczi MA, Homsher E & Trentham DR (1984). The kinetics of magnesium adenosine triphosphate cleavage in skinned muscle fibres of the rabbit. *J Physiol* **352**, 575–599.

Fitzsimons DP, Patel JR, Campbell KS & Moss RL (2001). Cooperative mechanisms in the activation dependence of the rate of force development in rabbit skinned skeletal muscle fibres. *J Gen Physiol* **117**, 133–148.

Greenberg MJ, Mealy TR, Watt JD, Jones M, Szczesna-Cordary D & Moore JR (2009). The molecular effects of skeletal muscle myosin regulatory light chain phosphorylation. *Am J Physiol Regul Integr Comp Physiol* **297**, R265–R274.

Greenberg MJ, Shuman H & Ostap EM (2014). Inherent force-dependent properties of beta-cardiac myosin contribute to the force-velocity relationship of cardiac muscle. *Biophys J* **107**, L41–L44.

Gu X, Liu X, Xu D, Li X, Yan M, Qi Y, Yan W, Wang W, Pan J, Xu Y, Xi B, Cheng L, Jia J, Wang K, Ge J & Zhou M (2010). Cardiac functional improvement in rats with myocardial infarction by up-regulating cardiac myosin light chain kinase with neuregulin. *Cardiovasc Res* **88**, 334–343.

Guccione JM, O'Dell WG, McCulloch AD & Hunter WC (1997). Anterior and posterior left ventricular sarcomere lengths behave similarly during ejection. *Am J Physiol* **272**, H469–H477.

Hanft LM, Korte FS & McDonald KS (2008). Cardiac function and modulation of sarcomeric function by length. *Cardiovasc Res* **77**, 627–636.

Hanft LM & McDonald KS (2010). Length dependence of force generation exhibit similarities between rat cardiac myocytes and skeletal muscle fibres. *J Physiol* **588**, 2891–2903.

He ZH, Bottinelli R, Pellegrino MA, Ferenczi MA & Reggiani C (2000). ATP consumption and efficiency of human single muscle fibres with different myosin isoform composition. *Biophys J* **79**, 945–961.

Hidalgo C, Wu Y, Peng J, Siems WF, Campbell KB & Granzier H (2006). Effect of diastolic pressure on MLC2v phosphorylation in the rat left ventricle. *Arch Biochem Biophys* **456**, 216–223.

Hooijman P, Stewart MA & Cooke R (2011). A new state of cardiac myosin with very slow ATP turnover: a potential cardioprotective mechanism in the heart. *Biophys J* **100**, 1969–1976.

Huang J, Shelton JM, Richardson JA, Kamm KE & Stull JT (2008). Myosin regulatory light chain phosphorylation attenuates cardiac hypertrophy. *J Biol Chem* **283**, 19748–19756.

Huxley AF (1957). Muscle structure and theories of contraction. *Prog Biophys Biophys Chem* **7**, 255–318.

Huxley AF & Simmons RM (1971). Proposed mechanism of force generation in striated muscle. *Nature* **233**, 533–538.

Ishijima A, Kojima H, Higuchi H, Harada Y, Funatsu T & Yanagida T (1996). Multiple- and single-molecule analysis of the actomyosin motor by nanometer-piconewton manipulation with a microneedle: unitary steps and forces. *Biophys J* **70**, 383–400.

Karabina A, Kazmierczak K, Szczesna-Cordary D & Moore JR (2015). Myosin regulatory light chain phosphorylation enhances cardiac beta-myosin in vitro motility under load. *Arch Biochem Biophys* **580**, 14–21.

Katz AM (2002). Ernest Henry Starling, his predecessors, and the "Law of the Heart". *Circulation* **106**, 2986–2992.

Kentish JC, ter Keurs HE, Ricciardi L, Bucx JJ & Noble MI (1986). Comparison between the sarcomere length-force relations of intact and skinned trabeculae from rat right ventricle. Influence of calcium concentrations on these relations. *Circ Res* **58**, 755–768.

Korte FS & McDonald KS (2007). Sarcomere length dependence of rat skinned cardiac myocyte mechanical properties: dependence on myosin heavy chain. *J Physiol* **581**, 725–739.

Levine RJ, Kensler RW, Yang Z, Stull JT & Sweeney HL (1996). Myosin light chain phosphorylation affects the structure of rabbit skeletal muscle thick filaments. *Biophys J* **71**, 898–907.

Mansfield C, West TG, Curtin NA & Ferenczi MA (2012). Stretch of contracting cardiac muscle abruptly decreases the rate of phosphate release at high and low calcium. *J Biol Chem* **287**, 25696–25705.

Metzger JM, Greaser ML & Moss RL (1989). Variations in cross-bridge attachment rate and tension with phosphorylation of myosin in mammalian skinned skeletal muscle fibres. Implications for twitch potentiation in intact muscle. *J Gen Physiol* **93**, 855–883.

Milani-Nejad N, Xu Y, Davis JP, Campbell KS & Janssen PM (2013). Effect of muscle length on cross-bridge kinetics in intact cardiac trabeculae at body temperature. *J Gen Physiol* **141**, 133–139.

Morano I (1992). Effects of different expression and posttranslational modifications of myosin light chains on contractility of skinned human cardiac fibres. *Basic Res Cardiol* **87** Suppl 1, 129–141.

Morano I, Osterman A & Arner A (1995). Rate of active tension development from rigor in skinned atrial and ventricular cardiac fibres from swine following photolytic release of ATP from caged ATP. *Acta Physiol Scand* **154**, 343–353.

Moss RL, Razumova M & Fitzsimons DP (2004). Myosin crossbridge activation of cardiac thin filaments: implications for myocardial function in health and disease. *Circ Res* **94**, 1290–1300.

Muthu P, Kazmierczak K, Jones M & Szczesna-Cordary D (2012). The effect of myosin RLC phosphorylation in normal and cardiomyopathic mouse hearts. *J Cell Mol Med* **16**, 911–919.

Nag S, Sommese RF, Ujfalusi Z, Combs A, Langer S, Sutton S, Leinwand LA, Geeves MA, Ruppel KM & Spudich JA (2015). Contractility parameters of human beta-cardiac myosin with the hypertrophic cardiomyopathy mutation R403Q show loss of motor function. *Sci Adv* **1**, e1500511.

Nishio H, Ichikawa K & Hartshorne DJ (1997). Evidence for myosin-binding phosphatase in heart myofibrils. *Biochem Biophys Res Commun* **236**, 570–575.

Nyitrai M & Geeves MA (2004). Adenosine diphosphate and strain sensitivity in myosin motors. *Philos Trans R Soc Lond B Biol Sci* **359**, 1867–1877.

Okamoto R, Kato T, Mizoguchi A, Takahashi N, Nakakuki T, Mizutani H, Isaka N, Imanaka-Yoshida K, Kaibuchi K, Lu Z, Mabuchi K, Tao T, Hartshorne DJ, Nakano T & Ito M (2006). Characterization and function of MYPT2, a target subunit of myosin phosphatase in heart. *Cell Signal* **18**, 1408–1416.

Olsson MC, Patel JR, Fitzsimons DP, Walker JW & Moss RL (2004). Basal myosin light chain phosphorylation is a determinant of Ca2+ sensitivity of force and activation dependence of the kinetics of myocardial force development. *Am J Physiol Heart Circ Physiol* **287**, H2712–H2718.

Pate E & Cooke R (1986). A model for the interaction of muscle cross-bridges with ligands which compete with ATP. *J Theor Biol* **118**, 215–230.

Patel JR, Pleitner JM, Moss RL & Greaser ML (2012). Magnitude of length-dependent changes in contractile properties varies with titin isoform in rat ventricles. *Am J Physiol Heart Circ Physiol* **302**, H697–H708.

Podolsky RJ, St Onge H, Yu L & Lymn RW (1976). X-ray diffraction of actively shortening muscle. *Proc Natl Acad Sci USA* **73**, 813–817.

Prakash YS, Cody MJ, Hannon JD, Housmans PR & Sieck GC (2000). Comparison of volatile anaesthetic effects on actin-myosin cross-bridge cycling in neonatal versus adult cardiac muscle. *Anaesthesiology* **92**, 1114–1125.

Prakash YS, Cody MJ, Housmans PR, Hannon JD & Sieck GC (1999). Comparison of cross-bridge cycling kinetics in neonatal vs. adult rat ventricular muscle. *J Muscle Res Cell Motil* **20**, 717–723.

Pulcastro HC, Awinda PO, Breithaupt JJ & Tanner BC (2016). Effects of myosin light chain phosphorylation on length-dependent myosin kinetics in skinned rat myocardium. *Arch Biochem Biophys* **601**, 56–68.

Regnier M, Lee DM & Homsher E (1998). ATP analogs and muscle contraction: mechanics and kinetics of nucleoside triphosphate binding and hydrolysis. *Biophys J* **74**, 3044–3058.

Regnier M, Martin H, Barsotti RJ, Rivera AJ, Martyn DA & Clemmens E (2004). Cross-bridge versus thin filament contributions to the level and rate of force development in cardiac muscle. *Biophys J* **87**, 1815–1824.

Regnier M, Rivera AJ, Chen Y & Chase PB (2000). 2-deoxy-ATP enhances contractility of rat cardiac muscle. *Circ Res* **86**, 1211–1217.

Rhodes SS, Camara AK, Aldakkak M, Heisner JS & Stowe DF (2015). Stretch-induced increase in cardiac contractility is independent of myocyte Ca^{2+} while block of stretch channels by streptomycin improves contractility after ischemic stunning. *Physiol Rep* **3**, e12486.

Sanbe A, Fewell JG, Gulick J, Osinska H, Lorenz J, Hall DG, Murray LA, Kimball TR, Witt SA & Robbins J (1999). Abnormal cardiac structure and function in mice expressing nonphosphorylatable cardiac regulatory myosin light chain 2. *J Biol Chem* **274**, 21085–21094.

Scruggs SB, Hinken AC, Thawornkaiwong A, Robbins J, Walker LA, de Tombe PP, Geenen DL, Buttrick PM & Solaro RJ (2009). Ablation of ventricular myosin regulatory light chain phosphorylation in mice causes cardiac dysfunction in situ and affects neighboring myofilament protein phosphorylation. *J Biol Chem* **284**, 5097–5106.

Sheikh F, Lyon RC & Chen J (2014). Getting the skinny on thick filament regulation in cardiac muscle biology and disease. *Trends Cardiovasc Med* **24**, 133–141.

Sheikh F, Ouyang K, Campbell SG, Lyon RC, Chuang J, Fitzsimons D, Tangney J, Hidalgo CG, Chung CS, Cheng H, Dalton ND, Gu Y, Kasahara H, Ghassemian M, Omens JH, Peterson KL, Granzier HL, Moss RL, McCulloch AD & Chen J (2012). Mouse and computational models link Mlc2v dephosphorylation to altered myosin kinetics in early cardiac disease. *J Clin Invest* **122**, 1209–1221.

Sonnenblick EH, Ross J, Jr., Covell JW, Spotnitz HM & Spiro D (1967). The ultrastructure of the heart in systole and diastole: changes in sarcomere length. *Circ Res* **21**, 423–431.

Stelzer JE, Larsson L, Fitzsimons DP & Moss RL (2006*a*). Activation dependence of stretch activation in mouse skinned myocardium: implications for ventricular function. *J Gen Physiol* **127**, 95–107.

Stelzer JE, Patel JR & Moss RL (2006*b*). Acceleration of stretch activation in murine myocardium due to phosphorylation of myosin regulatory light chain. *J Gen Physiol* **128**, 261–272.

Stracher A (1969). Evidence for the involvement of light chains in the biological functioning of myosin. *Biochem Biophys Res Commun* **35**, 519–525.

Sweeney HL & Stull JT (1990). Alteration of cross-bridge kinetics by myosin light chain phosphorylation in rabbit skeletal muscle: implications for regulation of actin-myosin interaction. *Proc Natl Acad Sci USA* **87**, 414–418.

Takagi Y, Homsher EE, Goldman YE & Shuman H (2006). Force generation in single conventional actomyosin complexes under high dynamic load. *Biophys J* **90**, 1295–1307.

Toepfer C, Caorsi V, Kampourakis T, Sikkel MB, West TG, Leung MC, Al-Saud SA, Macleod KT, Lyon AR, Marston SB, Sellers JR & Ferenczi MA (2013). Myosin regulatory light chain (RLC) phosphorylation change as a modulator of cardiac muscle contraction in disease. *J Biol Chem* **288**, 1346–1354.

Ueno H & Harrington WF (1981). Cross-bridge movement and the conformational state of the myosin hinge in skeletal muscle. *J Mol Biol* **149**, 619–640.

Wang YP & Fuchs F (1995). Osmotic compression of skinned cardiac and skeletal muscle bundles: effects on force generation, Ca^{2+} sensitivity and Ca^{2+} binding. *J Mol Cell Cardiol* **27**, 1235–1244.

Warren SA, Briggs LE, Zeng H, Chuang J, Chang EI, Terada R, Li M, Swanson MS, Lecker SH, Willis MS, Spinale FG, Maupin-Furlowe J, McMullen JR, Moss RL & Kasahara H (2012). Myosin light chain phosphorylation is critical for adaptation to cardiac stress. *Circulation* **126**, 2575–2588.

Wolff MR, McDonald KS & Moss RL (1995). Rate of tension development in cardiac muscle varies with level of activator calcium. *Circ Res* **76**, 154–160.

Yuan CC, Muthu P, Kazmierczak K, Liang J, Huang W, Irving TC, Kanashiro-Takeuchi RM, Hare JM & Szczesna-Cordary D (2015). Constitutive phosphorylation of cardiac myosin regulatory light chain prevents development of hypertrophic cardiomyopathy in mice. *Proc Natl Acad Sci USA*.

Additional information

Competing interests

The authors declare that they have no competing interests.

Author contributions

All data were collected at Imperial College London in the laboratory of Professor Michael A Ferenczi. CNT, TGW and MAF conceived and designed the experiments. CNT and MAF collected and analysed data. CNT, TGW and MAF interpretated data and produced the manuscript.

Funding

The present study was supported by Wellcome Trust Grant 091460/Z/10/Z.

Acknowledgements

We thank Dr Marco Caremani, Dr Andrey Tsaturyan and Dr Sergey Beshitsky for production and guidance regarding the maintenance of the temperature-jump apparatus. We also thank Dr Valentina Caorsi, Professor Nancy Curtin and Professor Roger Woledge for thoughtful discourse and guidance during the experiments.